Hindawi
Advances in Materials Science and Engineering
Volume 2018, Article ID 8951495, 5 pages
https://doi.org/10.1155/2018/8951495

Research Article

Transient Dynamics of Stimulated Raman Scattering in Gas-Filled Hollow-Core Photonic Crystal Fibers

Yashar E. Monfared

Department of Physics and Atmospheric Sciences, Dalhousie University, B3H 4R2 Halifax, NS, Canada

Correspondence should be addressed to Yashar E. Monfared; y.monfared@dal.ca

Received 15 June 2018; Revised 25 October 2018; Accepted 25 November 2018; Published 13 December 2018

Academic Editor: Andrey E. Miroshnichenko

A theoretical and numerical investigation of transient dynamics of stimulated Raman scattering (SRS) inside gas-filled hollow-core photonic crystal fibers (HCPCFs) is reported here. A clear link between the transient dynamics and the coherent memory of the SRS interaction is demonstrated. In addition, the role of pulse width, pump power, fiber length, and gaseous medium in the transient dynamics of SRS in HCPCFs is discussed. It is shown that the coherent memory can serve as a convenient parameter to control the SRS propagation regime.

1. Introduction

Hollow-core photonic crystal fibers (HCPCFs) are a class of photonic crystal fibers (PCFs) [1–3] which can guide the light in a hollow core or a core filled with gases [4]. This hollow-core usually is surrounded by a microstructured cladding which consists of air holes [4]. HCPCFs are extraordinaryly efficient for realizing resonance and near-resonance light-light and light-matter interactions due to long interaction length, small effective area, and the ability to suppress higher order modes [5, 6]. In optical physics, resonance and near-resonance interactions are usually modelled through either two-level amplification (TLA) or stimulated Raman scattering (SRS) process [7]. SRS process can be viewed as absorption of a photon from the pump pulse at frequency ω_p and the emission of a photon at Stokes frequency ω_s [8]. The difference in energy is taken up by molecular vibrations. Thus, SRS provides energy gain at the Stokes frequency at the expense of the pump. Generation of SRS in gaseous media, especially in HCPCFs, is of great theoretical and experimental interest [9, 10]. The Raman scattering effect can be separated into three regimes: spontaneous, stimulated transient, and stimulated steady-state [7]. The combination of the specific characteristics of HCPCFs, high intensity laser sources and gaseous media, has lead to the observation of quasi-CW SRS where the Raman transient regime extended to nanosecond-long pulses [11]. There are a number of publications that try to characterize and control transient regime of SRS. For example, the self-similar evolution in the highly transient regime of SRS in hydrogen-filled HCPCF theoretically and experimentally investigated by Nazarkin et al. [12]. Couny et al. [11] show the possibility of controlling transient regime of SRS by adjusting gas pressure and interaction length of HCPCF.

Usually, a transient regime of pulse propagation is when the pulse duration is shorter than the phase relaxation time T_2 of an atomic or molecular transition [12]. However, we should exercise caution employing this usual rule of thumb criterion [13]. This definition is based on quantum SRS theory in the undepleted pump approximation, and it can be extremely limiting in the nonlinear domain [13]. In fact, transient dynamics have been clearly illustrated in the recent SRS experiments with pulses as long as or even longer than the Raman relaxation time [12]. Thus, instead of using pulse duration which is not a promising parameter for determining transient regime of SRS, the concept of coherent memory is employed to characterize different propagation regimes.

In SRS, the coherent memory (Γ_c) is controlled by relative magnitudes of a characteristic SRS interaction time

(T_{SRS}) and the Raman medium relaxation time (T_2). Thus one can define the coherent memory parameter as $\Gamma_c = T_2/T_{SRS}$. We previously showed that coherent memory determines the extent of system memory and the system proximity to the integrability limit ($\Gamma_c \longrightarrow \infty$) [13, 14]. This paper proposes a comprehensive study of the transient dynamics in SRS in HCPCFs filled with different gases. The results suggest that the transient regime of SRS can indeed be controlled via the coherent memory parameter. This research opens possibilities for the generation of SRS in the transient regime with ultralong laser pulses and/or low-power pump sources.

2. Theoretical Framework

In this paper, a case of co-propagating Stokes and pump pulses in which all molecules of gaseous medium are in their ground states before excitation is considered. It should be noted that initial pump pulse was considered to be strong (high intensity) and initial Stokes was considered to be weak (nearly zero intensity). It is also assumed that the hollow-core fiber is designed to only allow the excitation of pump and fundamental Stokes modes. For simplicity, all parameters (including distance and time) scaled to characteristic SRS interaction time (T_{SRS}) and characteristic SRS interaction length (L_{SRS}). T_{SRS} can be defined as follows [13, 14]:

$$T_{SRS} = \frac{2\hbar\varepsilon_0 c n_p}{\alpha_{eff} I_{p0}}, \tag{1}$$

whereas L_{SRS} can be introduced as follows [13, 14]:

$$L_{SRS} = \left(\frac{2\varepsilon_0 c}{N\alpha_{eff}}\right)\sqrt{\frac{n_p n_s}{\omega_p \omega_s}}, \tag{2}$$

where $\omega_{s,p}$ is the angular frequencies of Stokes and pump, $n_{s,p}$ is the linear refractive indices of Stokes and pump, $\hbar$ is the reduced Planck constant, c is the speed of light in vacuum, I_{p0} is the average peak pump intensity, N is the density of gas molecules, ε_0 is the vacuum permittivity, and $\alpha_{eff} = (1/\hbar)\sum_i (d_{3i} d_{i1}/\omega_{i3} + \omega_{i1} - \omega_p - \omega_s)$ is a Raman transition dipole matrix element [15, 16]. The governing dimensionless SRS equations can be therefore written as follows [13, 14]:

$$\begin{aligned} \partial_Z \varepsilon_p &= ik\sigma\varepsilon_s, \\ \partial_Z \varepsilon_s &= ik^{-1}\sigma^* \varepsilon_p, \\ \partial_T \sigma &= -\Gamma_c^{-1}\sigma + i\varepsilon_p \varepsilon_s^*, \end{aligned} \tag{3}$$

where $\varepsilon_{s,p}$ is the dimensionless Stokes and pump amplitudes and $k = \sqrt{\omega_p n_s/\omega_s n_p}$. We have also considered the following normalization for propagation distance and time: $Z = z/L_{SRS}$ and $T = t/T_{SRS}$.

Finally, one should construct input Stokes and pump pulses. To enhance the SRS efficiency we have to maximize the pump and Stokes pulse intensity overlap. To this end, it is assumed that copropagating weak Stokes and strong pump pulses have the same durations, same Gaussian shape, and the same peak time, $T_p = T_s = T_0$. We previously studied the same SRS propagation equations using stochastic initial conditions and partially coherent pulses [14]. We showed that near-resonant SRS interaction is an ideal model to study extreme events due to potential noise transfer dynamics [13]. Here, we aim at studying a completely different phenomenon which includes the effect of pulses, gaseous medium (type of the gas), and fiber length on the propagation dynamics and transient regime of SRS. Therefore, we use a different set of initial conditions (coherent input pulses instead of partially coherent pulses) for our study. The dimensionless initial conditions can be written as follows:

$$\begin{aligned} E_p(T,0) &= e^{-T^2/2T_0^2}, \\ E_s(T,0) &= \sqrt{\frac{n_p I_{s0}}{n_s I_{p0}}} e^{-T^2/2T_0^2}. \end{aligned} \tag{4}$$

3. Numerical Results and Discussion

As a practical realization of the system, we consider a 10 mm long gas-filled HCPCF with typical parameters representative of the HCPCFs previously designed for SRS experiments [12]. The HCPCF has a narrow-band low-loss transmission window. Therefore, only the pump and first Stokes modes can copropagate in the HCPCF. Hydrogen is one of the best gaseous media for SRS generation due to its strong vibrational Raman modes, and it is widely used in Raman experiments [6, 8, 11]. Therefore, we mainly used hydrogen-filled HCPCF for our simulations.

We solved Maxwell-Bloch equations using numerical Runge–Kutta and Euler methods to see the evolution of Stokes and pump pulse profiles. We take the Raman transition dipole matrix element and relaxation time of hydrogen in the HCPCF to be $\alpha_{eff} = 0.85 \times 10^{-25}$ cm^{-3} and γ^{-1} = 5 ns at 1 bar, respectively [8, 10]. Note that the medium relaxation time (T_2) is inversely proportional to the total gas pressure. Thus one can use pressure as a controlling parameter in the SRS experiments in gas-filled HCPCFs. First, we examine Stokes pulse propagation in a 10 mm long HCPCF filled with hydrogen with different coherent memories: $\Gamma_c \ll 1$, $\Gamma_c \approx 1$, and $\Gamma_c \gg 1$. In order to achieve different memories, we choose a narrow linewidth laser delivering 100 ns, 15 ns, and 0.7 ns pulses of a 100 μJ energy as the pump while the Stokes pulse power is equal to 10 W. The corresponding coherent memory values are Γ_c = 0.4, Γ_c = 2, and Γ_c = 60, respectively. The reason we choose these specific values is the fact that each value corresponds to a different propagation regime of SRS, Γ_c = 0.4 corresponds to $\Gamma_c \ll 1$ 1 or steady-state regime, Γ_c = 2 corresponds to $\Gamma_c \approx 1$ which is the fairly transient regime, and Γ_c = 60 corresponds to $\Gamma_c \gg 1$ or highly transient regime. As we can see in Figure 1, by increasing coherent memory of SRS interaction, we move from a steady-state regime in Figure 1(a) to fairly transient regime in Figure 1(b) and then highly transient regime in Figure 1(c).

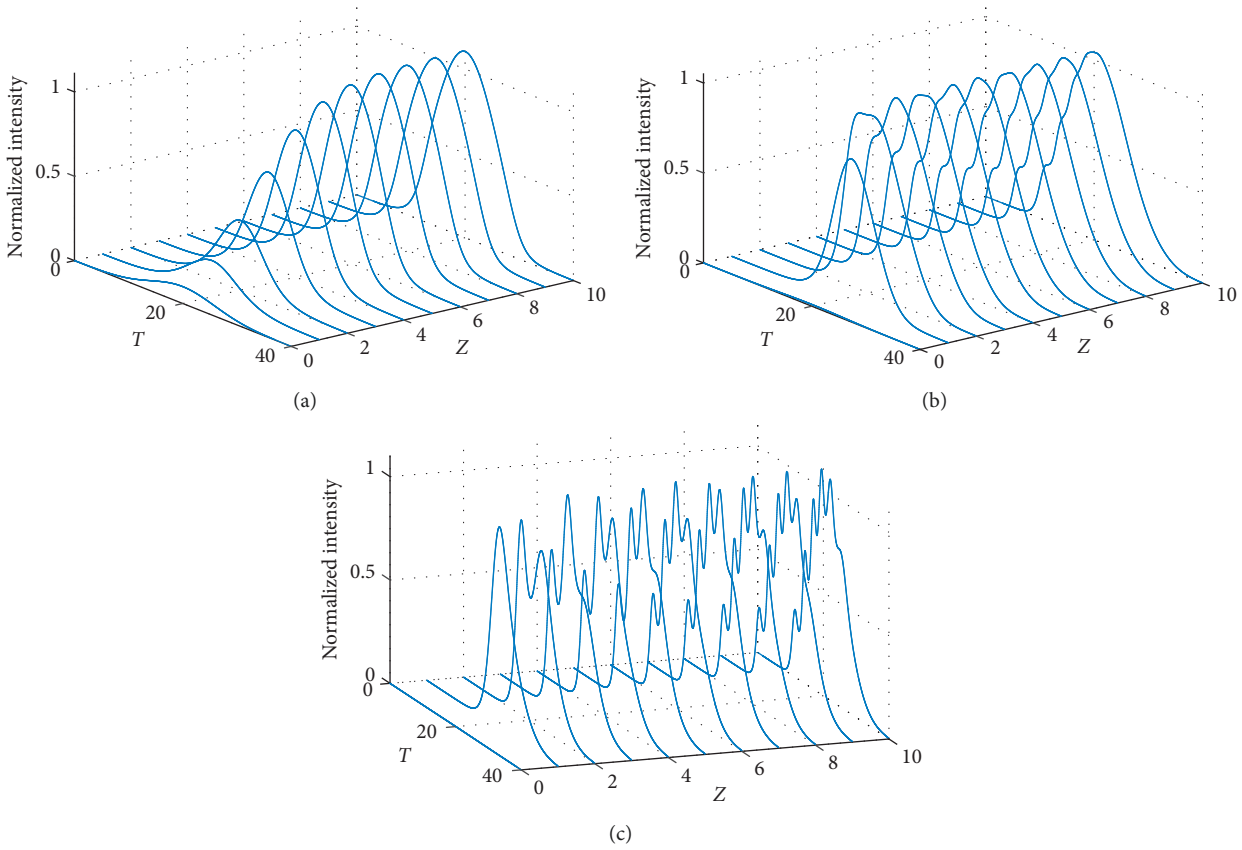

FIGURE 1: Normalized intensity fluctuations of Stokes pulse with (a) $\Gamma_c = 0.4$, (b) $\Gamma_c = 2$, and (c) $\Gamma_c = 60$, as functions of time and propagation distance.

These results clearly show the important role of coherent memory in transient dynamics of SRS in gas-filled HCPCFs. Another interesting point about this figure is the required interaction length for different case scenarios. In steady-state regime, the Stokes pulse need more time to reach the final stage of process (steady-state). Therefore, the fiber needs to be longer (in our case, $Z \approx 5$). However, in fairly transient and highly transient regimes, the Stokes pulses can reach the final stage pretty quickly ($Z \approx 1$). In late stage, we can see coherent fluctuations in the amplitude of Stokes pulse which clearly shows transient dynamics in the late stage of SRS with large coherent memory (Figure 1(c)). It can be inferred from Figure 1 that the value of Γ_c controls the propagation regime of Stokes and pump pulses in SRS. For $\Gamma_c \ll 1$, the SRS is quasi-CW and for $\Gamma_c \gg 1$, the SRS is highly transient with an extremely long memory time. Therefore, $\Gamma_c \approx 1$ is the boundary between quasi-CW and transient regime of SRS.

To further examine the transient dynamics in the case of large coherent memory, evolution of Stokes and pump pulses with a coherent memory of $\Gamma_c = 60$ is studied. The normalized intensities of the pump and Stokes pulses at several propagation distances are depicted in Figure 2. At the input of the fiber (Figure 2(a)), we have strong pump and weak Stokes pulses. As pulses start to propagate in the fiber, the Stokes pulse intensity grows at the expense of the pump (Figure 2(b)), and this is the early-stage of SRS process. In Figure 2(c), the pulses continue to propagate in the fiber, coherent oscillations show up, and this is the late stage of SRS process. These characteristic oscillations experienced by both intensity profiles clearly show a transient SRS regime. In Figure 2(d), we can see intensity profile of both Stokes and pump pulses at the output of the fiber which indicates a highly transient dynamics of SRS process at this stage.

Next, the role of pulse width on coherent memory is studied in detail using three different gases inside the core of the fiber and with a 100 μJ pump energy. As we mentioned before, hydrogen is the widely used gas in the previous Raman experiment. However, we consider two more type of gases to be able to compare the effect of coherent memory in each case. In our calculations, we consider hydrogen (H_2), nitrogen (N_2), and methane (CH_4) under the same pressure (1 bar). For N_2 and CH_4, the values of T_2 and α_{eff} are estimated from [17–20]. From Figure 3, one can clearly see why H_2 is simply more efficient in SRS experiments in gaseous media. The amount of coherent memory for H_2 is nearly 4 times larger than N_2 and 40 times larger than CH_4 for 1 ns pulses. According to Figure 3, by increasing pulse width, the coherent memory decreases significantly. For pulses with 20 ns width, the coherent memory of H_2 is nearly 16 times smaller than that of 1 ns pulses ($\Gamma_c = 5$ for 20 ns pulses compared to $\Gamma_c = 82$ for 1 ns pulses). We infer that the pulse width has a significant effect on the transient dynamics of SRS filled with different gases. This reduction in coherent

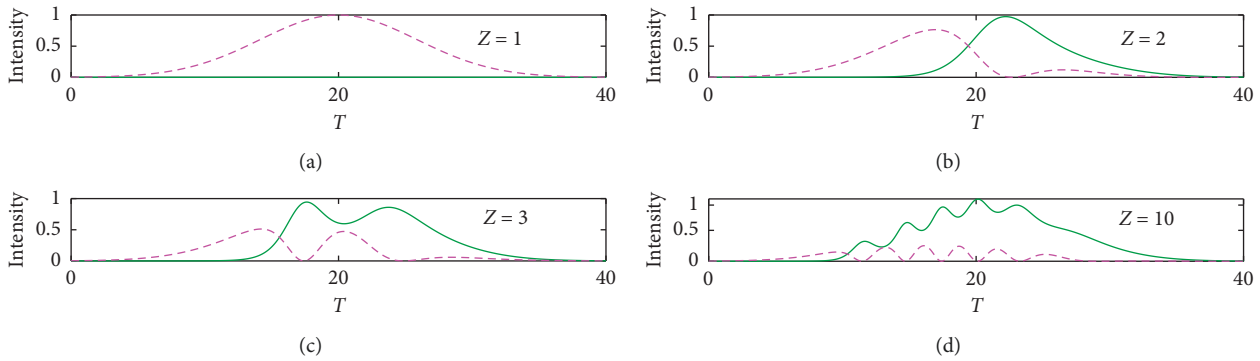

FIGURE 2: Normalized intensity profiles of the pump (dashed magenta) and Stokes (solid green) pulses at several propagation distances. The coherent memory parameter is taken to be $\Gamma_c = 60$.

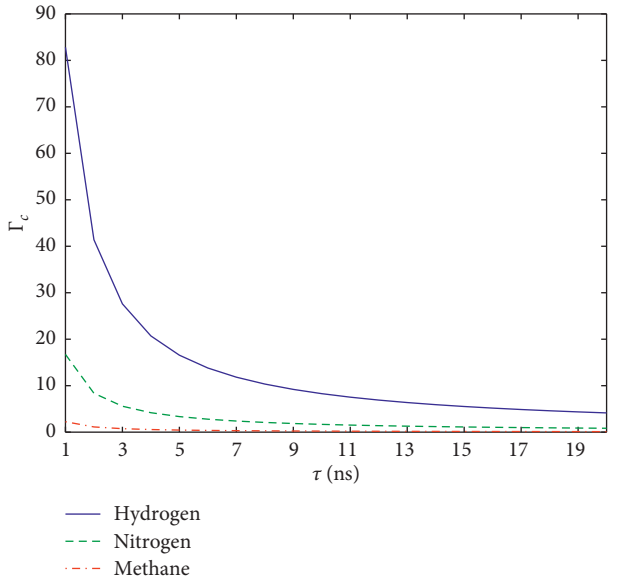

FIGURE 3: Coherent memory of SRS interaction with a pump energy of 200 μJ as a function of pulse width for three different gases.

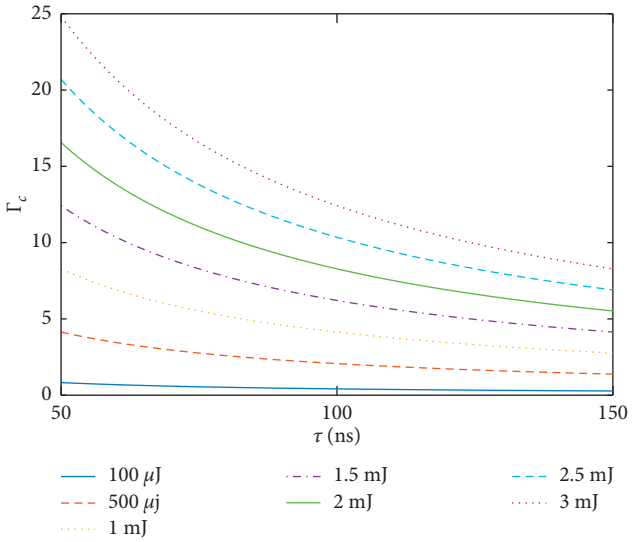

FIGURE 4: Coherent memory of SRS interaction as a function of pulse width for hydrogen-filled HCPCF with different pump energy levels.

memory of SRS interaction is more significant for H_2 and N_2 than for CH_4.

Furthermore, it is possible to achieve long coherent memory even with pulses longer than 10 ns. Figure 4 shows the relation between coherent memory and pulse width for different pump energies in a H_2-filled HCPCF at 1 bar pressure. It can be clearly inferred from Figure 4 that as we increase the pump energy, the coherent memory increases as well. For instance, one can achieve highly transient SRS ($\Gamma_c \approx 13$) with 50 ns pulses and a pump energy of only 1.5 mJ. This pulse width is extremely longer than that of the Raman relaxation time of hydrogen molecule in HCPCF (50 ns pulse width compared to 5 ns Raman relaxation time). In fact, it is even possible to achieve transient regime with pulses longer than 100 ns by simply increasing the pump energy to higher levels. For example, one can achieve highly transient regime of SRS with 100 ns and 150 ns pulses by simply increasing the pump energy to 2 mJ and 3 mJ, respectively.

4. Conclusion

In this paper, different propagation regimes of SRS in gas-filled HCPCFs are theoretically and numerically investigated. Coherent oscillations in the amplitude of both Stokes and pump pulses in the late stage of SRS process is studied as a signature of transient regime of pulse propagation. The latter can be conveniently controlled by adjusting the coherent memory of SRS interaction via pump energy, pulse width, and even gas pressure. For $\Gamma_c \ll 1$, the SRS is steady-state, and for $\Gamma_c \gg 1$, the SRS is highly transient with an extremely long memory time. Therefore, $\Gamma_c \approx 1$ is the boundary between steady-state and transient regime of SRS. Therefore our findings establish a clear link between coherent memory and transient dynamics in SRS inside a gas-filled HCPCF.

Data Availability

The data used to support the findings of this study are included within the article.

Conflicts of Interest

The author declares that there are no conflicts of interest regarding the publication of this paper.

References

[1] C. Zhang, Z. Zhang, X. Xu, and W. Cai, "Thermally optimized polarization-maintaining photonic crystal fiber and its FOG application," *Sensors*, vol. 18, no. 2, p. 567, 2018.

[2] Y. E. Monfared and S. A. Mojtahedinia, "Highly birefrigent photonic crystal fiber with high negative dispersion for broadband dispersion compensation," *Optik*, vol. 125, no. 20, pp. 5969–5972, 2014.

[3] Y. E. Monfared, A. Mojtahedinia, A. R. Maleki Javan, and A. R. Monajati Kashani, "Highly nonlinear enhanced-core photonic crystal fiber with low dispersion for wavelength conversion based on four-wave mixing," *Frontiers of Optoelectronics*, vol. 6, no. 3, pp. 297–302, 2013.

[4] F. Gérôme, R. Jamier, J.-L. Auguste, G. Humbert, and J.-M. Blondy, "Simplified hollow-core photonic crystal fiber," *Optics Letters*, vol. 35, no. 8, pp. 1157–1159, 2010.

[5] F. Benabid, P. St, and J. Russell, "Hollow-core photonic crystal fibers: progress and prospects," *Proceedings of SPIE*, vol. 5733, p. 5733, 2005.

[6] R. Jamier, F. Gerome, G. Humbert, J. L. Auguste, J. M. Blondy, and F. Benabid, "Prospects on Hollow-core Photonic Crystal Fibers for unconventional fibered laser sources," in *Proceedings of 13th International Conference on Transparent Optical Networks*, pp. 1–5, Stockholm, Sweden, June 2011.

[7] L. Allen and J. H. Eberly, *Optical Resonance and Two-Level Atoms*, Dover Publications, US, 1987.

[8] M. F. Ferreira, *Nonlinear effects in optical fibers*, Wiley-OSA, Mineola, NY, USA, 2011.

[9] M. Ziemienczuk, A. M. Walser, A. Abdolvand, P. S. J. Russell, and J. Russell, "Intermodal stimulated Raman scattering in hydrogen-filled hollow-core photonic crystal fiber," *Journal of the Optical Society of America B*, vol. 29, no. 7, pp. 1563–1568, 2012.

[10] F. Belli, A. Abdolvand, J. C. Travers, P. St, and J. Russell, "Control of ultrafast pulses in a hydrogen-filled hollow-core photonic-crystal fiber by Raman coherence," *Physical Review A*, vol. 97, no. 1, article 013814, 2018.

[11] F. Couny, O. Carraz, and F. Benabid, "Control of transient regime of stimulated Raman scattering using hollow-core PCF," *Journal of the Optical Society of America B*, vol. 26, no. 6, pp. 1209–1215, 2009.

[12] A. Nazarkin, A. Abdolvand, A. V. Chugreev, P. St, and J. Russell, "Direct observation of self-similarity in evolution of transient stimulated Raman scattering in gas-filled photonic crystal fibers," *Physical Review Letters*, vol. 105, no. 17, article 173902, 2010.

[13] Y. E. Monfared and S. A. Ponomarenko, "Non-Gaussian statistics of extreme events in stimulated Raman scattering: the role of coherent memory and source noise," *Physical Review A*, vol. 96, no. 4, article 043817, 2017.

[14] Y. E. Monfared and S. A. Ponomarenko, "Non-Gaussian statistics and optical rogue waves in stimulated Raman scattering," *Optics Express*, vol. 25, no. 6, pp. 5941–5950, 2017.

[15] F. Belli, A. Abdolvand, W. Chang, J. C. Travers, P. S. J. Russell, and J. Russell, "Vacuum-ultraviolet to infrared supercontinuum in hydrogen-filled photonic crystal fiber," *Optica*, vol. 2, no. 4, p. 292, 2015.

[16] F. Flora and L. Giudicotti, "Complete calibration of a Thomson scattering spectrometer system by rotational Raman scattering in H2," *Applied Optics*, vol. 26, no. 18, pp. 4001–4008, 1987.

[17] H. Ory and H. T. Yura, *Rayleigh and Raman Scattering in Molecular Nitrogen*, RM-4664-ARPA, RAND Corporation, Santa Monica, CA, USA, 1965.

[18] C. K. Miller, B. J. Orr, and J. F. Ward, "An interacting segment model of molecular electric tensor properties: application to dipole moments, polarizabilities, and hyperpolarizabilities for the halogenated methanes," *Journal of Chemical Physics*, vol. 74, no. 9, pp. 4858–4871, 1981.

[19] D. R. Miller and R. P. Andres, "Rotational relaxation of molecular nitrogen," *Journal of Chemical Physics*, vol. 46, no. 9, pp. 3418–3423, 1967.

[20] A. Chugreev, A. Nazarkin, A. Abdolvand et al., "Manipulation of coherent Stokes light by transient stimulated Raman scattering in gas filled hollow-core PCF," *Optics Express*, vol. 17, no. 11, pp. 8822–8829, 2009.